Modelling cortical folding pattern formation of the brain with a Turing system

Hurdal, M.K. [1] and D.A. Striegel [1]

[1] *Department of Mathematics, Florida State University, Tallahassee, Florida, U.S.A. 32306-4510*
Email: mhurdal@math.fsu.edu

Abstract: The folding patterns of the brain vary dramatically across species. Moreover, the location of sulcal (valley) and gyral (ridge) folds differ considerably in terms of their size, shape and extent even within a species. A paradigm for cortical pattern formation within or across species has not become apparent. Discussions as to how cortical folding patterns occur have recently emerged in the literature. Current proposals describe folding through local interactions and include a mechanistic model and a cellular model. In this paper we present a simple and elegant mathematical model that offers a possible explanation as to the location of cortical fold formation. Our model takes into account global cortex characteristics and can be used to model folds across species as well as specific diseases that can occur in human brain folding patterns.

Our model uses a Turing reaction-diffusion system to model cortical folding. Turing systems have been used to study pattern formation in a wide variety of biological applications using 1D, 2D and spherical domains. Turing systems use an activator and inhibitor and under certain conditions, a steady state will emerge causing a pattern to form. We employ phenomenological kinetic equations of Barrio-Varea-Maini (BVM) for our reaction-diffusion model.

Due to the shape of the lateral ventricle (LV) in the cortex, we use a prolate spheroidal domain. A prolate spheroid is created by rotating an ellipse about its major axis. The focal distance of the prolate spheroid is determined by the major and minor axes. It has been suggested that cortical pattern formation is due to regional patterns of intermediate progenitor (IP) cells in the subventricular zone (SVZ) of the cortex. During cortical development certain radial glial cells in the ventricular zone (VZ) are activated to create IP cells that travel to the SVZ. These areas lead to neuron amplification and gyrus formation. Our model approximates the shape of the LV with a prolate spheroid and the VZ with a prolate spheroidal surface.

With our model we are able to predict cortical folding patterns that correlate with cortical observations. As we increase the scaling of our prolate spheroidal domain we observe more elaborate cortical patterns. Additionally, our simulations reveal that the occurrence of the directionality of primary sulci occurring in different species can be accounted for by using the focal distance parameter in our model. Changing the focal distance corresponds to changing the shape of the VZ, resulting in changes in the location and type of sulcal pattern observed. By encapsulating global cortex shape characteristics, our model also has the ability to predict why the cortex of certain species may have little or no folding and it can link the evolutionary development of cortical sulcal formation to the eccentricity of the lateral ventricle.

Our model is also able to elucidate reasons as to how certain diseases in cortical pattern formation may occur. Polymicrogyria is a cortical malformation disease that occurs in the human brain and results in an over abundance of cortical folding. This disease is thought to be a neuronal migration disorder and can result in developmental delays, seizures and facial disfigurations. Numerical simulations with our model have enabled us to better understand cortical characteristics which can lead to excessive cortical folding. This application of our model, coupled with patient magnetic resonance imaging (MRI) data of the cortex, may explain how certain cortical pattern formation disease processes develop.

By applying prolate spheroidal harmonics to a Turing system, we have developed a chemically-based mathematical model that predicts the order and directionality of sulcal pattern formation across species based on global shape characteristics. Our model is able to predict and explain the consistency in pattern formation across species. Additionally our model is able to elucidate global cortex characteristics that may result in cortical pattern formation diseases.

Keywords: Brain, cortical folding, pattern formation, gyrus, polymicrogyria, prolate spheroid, reaction diffusion system, sulcus, Turing pattern

1. INTRODUCTION

A paradigm for the development of cortical folding patterns in the brain remains an open question. The valleys (sulci) and ridges (gyri) of the folding patterns vary considerably within and across species. A number of hypotheses have been proposed to explain cortical folding, but no consensus has been reached. Current theories tend to be based on local interactions in the cortex. One theory is mechanistic, and is the axonal tension hypothesis (Van Essen, 1997). Tension along the white matter axons is thought to be the basis for cortical folding. Axon tension pulls strongly interconnected regions together so that the axonal distance within the white matter is reduced, leading to an outward fold which forms a gyrus. Weakly interconnected cortical regions can be separated by greater axonal distances and so the tension is not as great, leading to inward folds and sulci formation. More recently, the intermediate progenitor (IP) hypothesis (Noctor et al., 2004), followed by the IP model (Kriegstein et al., 2006) have been put forward to explain cortical folding. These hypotheses are cellular based. It is known that as the cortex develops, it is initially composed of a layer of proliferative cells lining the lateral ventricle called the ventricular zone (VZ). Subsequently, a second proliferative layer, called the subventricular zone (SVZ), forms. IP cells, which are located in the SVZ, can amplify the number of neurons that travel to the cortex. The IP model suggests that only subsets of the IP cells create a local amplification, which results in gyrus formation.

In this paper we present a mathematical model to explain how IP cell subsets are distributed spatially and temporally in the developing cortex. We give details of a Turing reaction-diffusion system to model cortical folding pattern formation. Turing systems have been used model a wide variety of complex pattern formation in biological systems, including fish patterns (Kondo, 1995), animal coat patterns (Murray, 2003), and bacteria (Varea, 1999). In the following sections we give details of our model and demonstrate that we are able to predict cortical folding patterns that correlate with cortical observations. We also describe how our model may be extended to provide a link between the concepts of the axonal tension hypothesis and the IP model. Additionally, we discuss how certain diseases in cortical pattern formation may occur and how patient data of the cortex may be used to refine this model.

2. THE MODEL

The IP hypothesis explains that during the development of the cortex, certain radial glial cells in the VZ are activated to create IP cells that travel to the SVZ. The lateral ventricle and VZ are critical components in the development of cortical pattern formation. Thus, we model the shape of the lateral ventricle with a prolate spheroid and the VZ with a prolate spheroidal surface. The direction of the major axis of the prolate spheroid corresponds to the major axis of the later ventricle. Using a prolate spheroidal domain enables the focal distance to model the eccentricity of the lateral ventricle.

In our model, we assume that activator and inhibitor reactants regulate IP cell production. Thus, we are able to using a Turing reaction-diffusion system as the basis of our model. Turing systems use an activator and inhibitor and under certain conditions, a steady state will emerge causing a pattern to form. Our mathematical model is chemically based and takes advantage of global characteristics of the cortex rather than local interactions.

2.1. Turing Systems

A Turing system is a reaction-diffusion system of two chemical morphogens representing an activator and an inhibitor. Two criteria need to be satisfied for a system to be a Turing reaction-diffusion system: i) the system is linearly stable in the absence of diffusion; ii) the system becomes linearly unstable when diffusion is present. In order to realistically capture biological phenomena, the reaction kinetics must be linear and nonlinear. We use the Barrio-Varea-Maini (BVM) Turing model (Barrio et al., 1999) because it does not assume any particular kinetic scheme and tries to capture the phenomenon of the pattern that forms. The BVM system is

$$u_t = d\delta\nabla^2 u + \alpha u(1 - r_3 v^2) + v(1 - r_2 u) \text{ and } v_t = \delta\nabla^2 v + \beta v\left(1 + \frac{\alpha r_3}{\beta}uv\right) + u(\gamma + r_2 v), \quad (1)$$

where u and v are the activator and inhibitors respectively at position $\boldsymbol{x}$ and time t and are centered around the steady state $(u_0, v_0) = (0, 0)$, d is the ratio of diffusion coefficients, δ is a positive constant that is inversely proportional to the domain scaling, the linear interaction parameters are represented by α, β and γ, and r_2 and r_3 represent the quadratic and cubic interaction parameters respectively. Expanding the reaction kinetics in a

Taylor series around the steady state and neglecting higher order terms leads to the following conditions that must be satisfied for the system to be a Turing system:

$$\alpha+\beta<0, \ \alpha\beta-\gamma>0, \ \delta d\beta + \delta\alpha > 0, \text{ and } \frac{(d\beta+\alpha)^2}{4d} > 0. \tag{2}$$

2.2. Prolate Spheroidal Surface

A prolate spheroid is created by rotating an ellipse about its major axis and has focal distance $f = \sqrt{a^2 - b^2}$, where a and b are the major and minor axes, respectively. Prolate spheroidal coordinates are expressed as (ξ, η, φ) where ξ is the radial term with $\xi \geq 0$, $\eta = \cos\theta$ where θ is the asymptotic angle with respect to the major axis with $-1 \leq \eta \leq 1$, and φ is the rotation term with $0 \leq \varphi \leq 2\pi$.

To examine Turing patterns on a prolate spheroidal surface, we solve the Helmholtz Equation, $\nabla^2 X + k^2 X = 0$ with respect to prolate spheroidal coordinates, where k is the eigenvalue and is determined by the domain. Using the BVM system, k^2 is related to the domain scaling and is determined to be $k^2 = \frac{d\beta+\alpha}{2d\delta}$. The Helmholtz Equation is separable in prolate spheroidal coordinates (Flammer, 1957) and so the solution can be written as $X = R(r)S(\xi)\Theta(\varphi)$, where R, S and Θ satisfy

$$\frac{d}{d\xi}\left[(\xi^2 -1)\frac{dR}{d\xi}\right] - \left[\lambda - \frac{k^2 f^2 \xi^2}{4} + \frac{m^2}{\xi^2 -1}\right]R = 0, \tag{3a}$$

$$\frac{d}{d\eta}\left[(1-\eta^2)\frac{dS}{d\eta}\right] + \left[\lambda - \frac{k^2 f^2 \eta^2}{4} - \frac{m^2}{1-\eta^2}\right]S = 0, \text{ and} \tag{3b}$$

$$\Theta'' + m^2\Theta = 0, \tag{3c}$$

where λ and m are constants. The solutions of R and S involve radial equations and Legendre Functions that contain parameters m and n and so they will be denoted R_{mn} and S_{mn}. The constant λ represents the spheroidal eigenvalues which also depend on m and n. It is also a function of $kf/2$ and will be denoted λ_{mn} for brevity. Note that m and n are the spheroidal harmonic indices.

As we are interested in a prolate spheroidal surface domain, we only consider solutions which are radially invariant, i.e. $\frac{dR}{d\xi} = 0$ for a prolate spheroid of constant radius $\xi = \xi_0$. Thus, Equation (3a) yields

$\lambda_{mn} - \frac{k^2 f^2 \xi_0^2}{4} + \frac{m^2}{\xi^2 -1} = 0$, which, after rearranging, leads to

$$k^2 = \frac{4}{f^2\xi_0^2}\left(\lambda_{mn} + \frac{m^2}{\xi^2 -1}\right), \text{ which we will write as } k^2 = A_{mn}. \tag{4}$$

The significance of Equation (4) is that it enables pattern formation to be predicted by relating a given domain scaling (controlled by k^2) and domain shape (the eccentricity of the prolate spheroid controlled by f) to the arising pattern (indicated by the spheroidal indices m and n). Further details of these derivations can be found in Striegel, 2009.

3. SIMULATIONS AND RESULTS

3.1. Numerical Simulations

We discretized the BVM Turing System in (1) using a Forward Euler (forward time, central space) method on a 34 x 68 grid with respect to θ and φ. Periodic boundary conditions with respect φ to were used and boundary conditions with respect to θ were chosen such that continuity around the north and south poles were preserved. The prolate spheroid surface radius, ξ_0, was selected so the prolate spheroidal shell conserves a surface area of 4π, similar to a unit sphere. Note that ξ_0 depends on the value of the focal distance f. Parameter values for (1) satisfy the conditions of (2) and were set as follows: $\alpha = 0.899$, $\beta = -0.91$,

$\gamma = -0.899$, $d = 0.5319$, $r_2 = 0$ and $r_3 = 3.5$. Parameter values for δ and f were varied to control the domain scale and domain shape.

3.2. Pattern Formation

The pattern that is formed can be described by the harmonic solution (m, n). Given a two tone color gradient such as black to copper, m corresponds to the number of copper (or black) spots traversing φ and n corresponds to m plus the number of shifts from copper to black (or black to copper) traversing θ for a fixed φ. Copper regions can be considered to be activated regions and black regions are non-activated regions (see Figures 1B, 1C). The arising pattern can be predicted by examining the solutions of Equation (4). Figure 1A plots A_{mn} for $n = 8, 9, 10$ and $m = 0, \ldots, n$ when the focal distance $f = 1$ (causing $\xi_0 = 2.164$). The asterisk located at $k^2 = 90$ corresponds to the curve A_{59}, meaning that a $(5, 9)$ pattern is predicted. Interestingly, when $k^2 = 90$ then $\delta = 0.00433$ and simulations of the pattern produced for this value of δ and for $f = 1$ do indeed correspond to a $(5, 9)$ pattern as illustrated in Figures 1B and 1C.
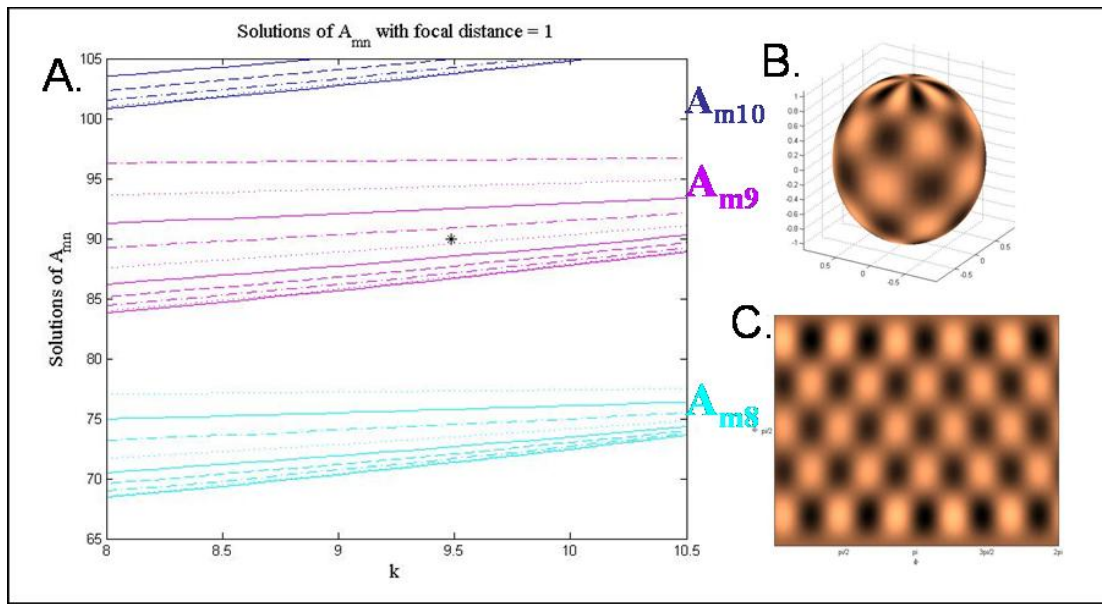

Figure 1: Prediction of Pattern Formation. A) A_{mn} versus k for $n = 8, 9, 10$ (different colors) and $m = 0, ..., n$ (different line styles). The asterisk at $A_{mn} = 90$ (i.e. $k^2 = 90$) corresponds to the curve A_{59} and predicts a $(5, 9)$ pattern. B) Simulation of equations in (1) projected on a prolate spheroid with $\delta = 0.00433$ (corresponding to $k^2 = 90$) and $f = 1$. C) Projection of B) onto a plane such that the left and right edges connect and the top (bottom) edge corresponds with the north (south) pole.

3.3. Transverse and Sectorial Patterns

A number of simulations were carried out that studied the role of domain scaling on the pattern formation of transverse and sectorial curves. Sectorial curves are formed when the spheroidal harmonic indices are equal. For example $(m, n) = (1, 1)$ forms one sectorial curve, $(2, 2)$ forms two sectorial curves, etc. Transverse curves are formed for spheroidal harmonic indices $(0, n)$ for n even. For example, $(0, 2)$ forms one transverse curve, $(0, 4)$ forms two transverse curves, etc. Examples of transverse and sectorial curves are shown in Figure 2.

Interestingly, as focal distance increases, the order in which transverse and sectorial curve formation changes (see Figure 3). As the domain scaling k^2 increases for $f = 4.5$, the harmonic A_{02} occurs first, followed by A_{11} and then A_{04} (see Figure 3A). This corresponds to a transverse pattern formed first followed by a sectorial pattern. When $f = 6.5$, as the domain scaling (k^2) increases, the harmonic A_{02} occurs first, followed by A_{04}, then A_{11} (see Figure 3B). This corresponds to two transverse patterns being formed before a sectorial pattern.
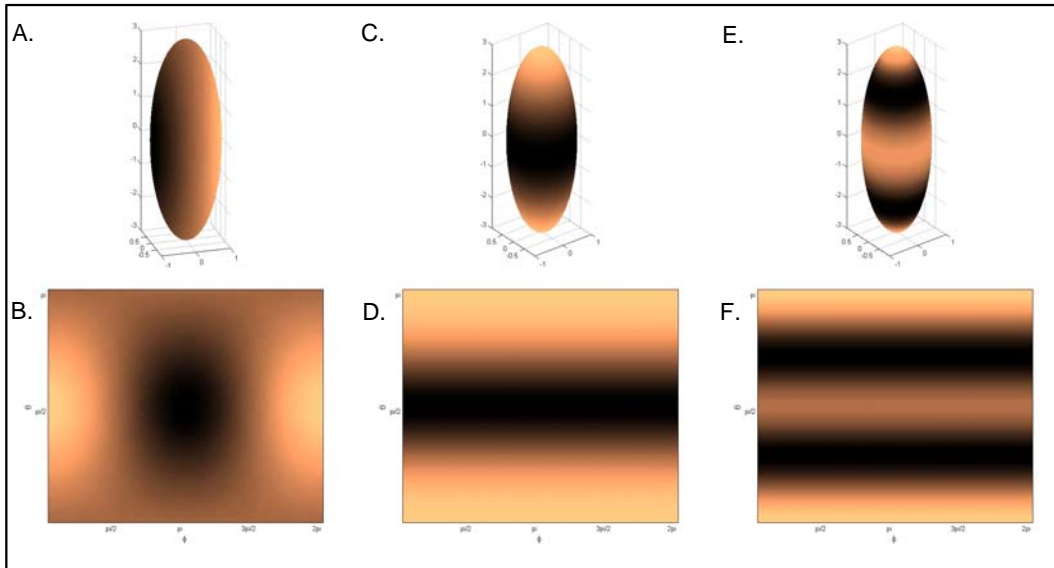
Figure 2. Transverse and Sectorial Curves. A) Prolate spheroidal harmonic (1, 1) corresponds to one sectorial curve formation. B) Projection of A) onto a plane such that the left and right edges connect and the top (bottom) edge corresponds with the north (south) pole. C) and D) Prolate spheroidal harmonic (0, 2) corresponds to the formation of one transverse ring and is projected onto a prolate spheroid and rectangle. E) and F) Prolate spheroidal harmonic (0, 4) corresponds to the formation of two transverse rings.
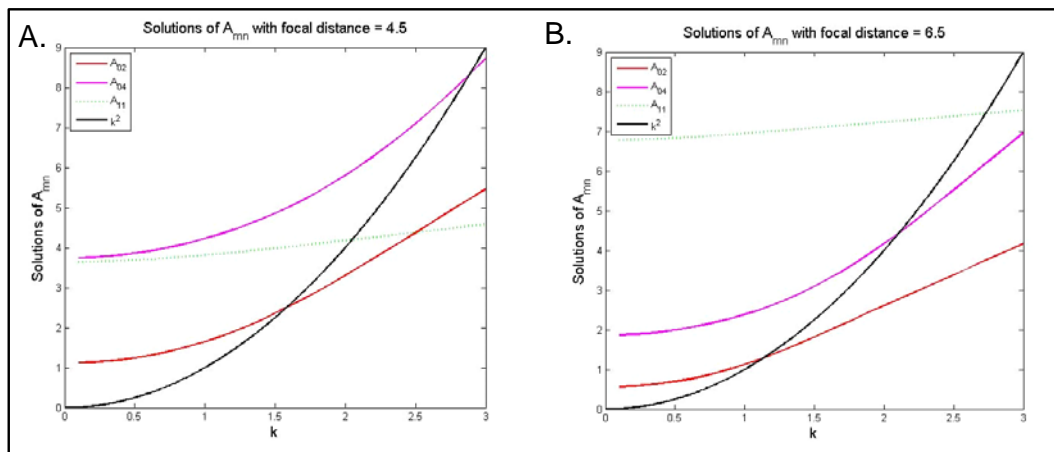

Figure 3. Effect of Focal Distance on Sectorial and Transverse Curve Formation. A) A_{mn} versus k for $f = 4.5$. Notice as k increases, the graph of k^2 intersects with the harmonic curves in the order of A_{02}, A_{11}, A_{04}. B) A_{mn} versus k for $f = 6.5$. The A_{mn} curves have shifted and now, as k increases, the order of intersection is A_{02}, A_{04}, A_{11}.

3.4. Multiple Sectorial Patterns

If focal distance is chosen to be small enough, then a scenario can arise where a sectorial curve is formed before any transverse curves. Simulation results indicate this to be true for focal distances between 1 and 3.7 (Striegel and Hurdal, 2009). If conditions are such that no transverse sulci are formed after the sectorial curve, then the domain becomes angularly invariant. In such a situation, as the domain scaling increases, greater numbers of sectorial curves are generated. This result is implied by Figure 1A. If only sectorial patterns are considered (which are given by A_{mn} for $m = n$), then as domain scaling (k^2) increases, the number of sectorial curves increases.

Simulations for this scenario correspond to solving the Helmholtz Equation in one dimension since our domain is angularly invariant. A small focal distance of $f = 1$ and a large domain scaling of $k^2 = 20$ generates

the results in Figure 4. Activated regions form when the amount of activator is positive (Figure 4A), resulting in multiple sectorial patterns forming (Figures 4B, 4C).
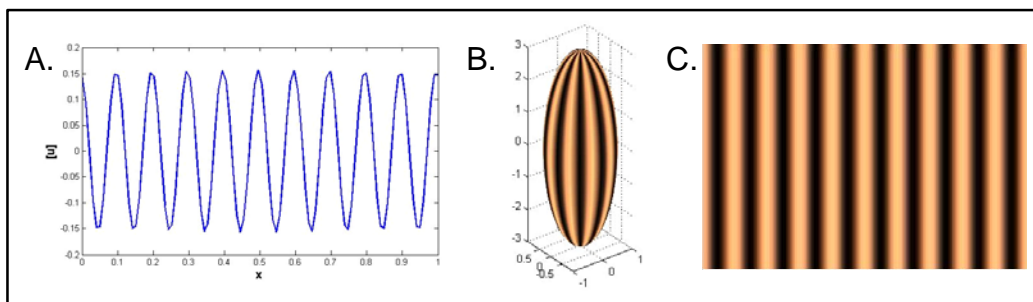

Figure 4. Formation of Multiple Sectorial Curves. Under certain conditions, a large domain scale ($k^2 = 20$) and small focal distance ($f = 1$) can lead to multiple sectorial curves forming. When the amount of activator is positive (Fig. A), activated (copper) regions are formed and lead to the pattern shown. Pattern projected on A) a prolate spheroid and B) a plane.

4. DISCUSSION AND CONCLUSIONS

Let us consider how prolate spheroidal harmonics may be framed in terms of cortical sulci of the brain. Sectorial sulci in the brain correspond to sulci that extend from the frontal lobe around the Sylvian fissure to the temporal lobe, matching the direction of the major axis of the prolate spheroid approximating the lateral ventricle. Examples of sectorial sulci include the calcarine sulcus and the cingulate sulcus. Transverse sulci correspond to rings around the VZ, and examples include the central and precentral sulcus.

In terms of IP cell production, a sulcus is formed when IP cells on either side of a sulcus are activated, causing the gyral banks on either side of a sulcus to be created. Activated (copper) regions of the spheroidal harmonic curves (see Figure 2) can be considered to be regions of activated IP cells, leading to gyrus formation. Inactivated regions would lead to sulcus formation.

We observed that as focal distance increased, a changed occurred in the order in which transverse and sectorial curves formed. The change from transverse to sectorial curves is of significance rather than the number of curves formed. Thus, focal distance affects the order in which curves, and hence sulci, are formed.

We offer two interpretations of these results, both of which correlate well with what is observed in the cortex.

One interpretation is related to evolution. As species have evolved, the cortex has expanded and the focal distances of the lateral ventricle and VZ have increased. The results of Figure 3 can be interpreted to mean that earlier in an evolutionary timeline when the lateral ventricle focal distances are smaller, the first transverse sulcus appears. Later in the evolutionary timeline, when the focal distances are larger, a second transverse sulcus appears. This is indeed what is observed in primates (see Figure 5). The first transverse sulcus can be interpreted as the formation of the calcarine sulcus, which is observed in both prosimian and anthropoid primates. However, prosimians, such as the lemur, are primitive primates and most are distinguished from higher primates by the absence of the central sulcus (Radinsky, 1975). The formation of a second transverse sulcus due to a larger focal distance as in Figure 3B can be interpreted as the formation of the central sulcus in higher order primates (see Figures 5C, 5D) due to the larger VZ focal distance. One example is the howler monkey.

Another interpretation is related to cortical disease. Polymicrogyria, meaning many small gyri, is a cortical disease in which there is an overproduction in the number of folds. It is characterized by an excessive number of small prominent convolutions spaced out by shallow and enlarged sulci. One
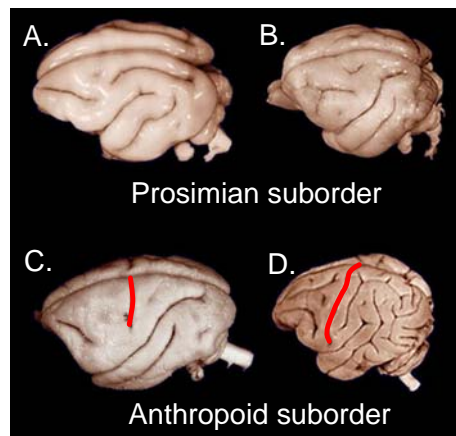

Figure 5. Prosimians versus Anthropoids. A) Ring-Tailed Lemur (Lemur catta). B) Slow Loris (Nycticebus coucang). C) Mantled Howler Monkey (Alouatta palliata). D) Lar Gibbon (Hylobates lar). The central sulcus is shown in red. Most prosimians do not have a central sulcus. Images adapted from http://www.brainmuseum.org.

form of polymicrogyria occurs with hydrocephalus (Colombani, 2006) and the enlarged sulci tend to be in the sectorial direction. Hydrocephalus causes the lateral ventricle to enlarge. The result is in an increase of domain scale. There is also a change in the aspect ratio of the major and minor axes of the prolate spheroid, resulting in a decrease in the focal distance. Under certain conditions, our model predicts that a decrease in the focal distance and an increase in the domain scale results in multiple sectorial sulci being formed (see Figure 4), and this is the pattern of folds observed in this particular form of polymicrogyria.

The application of our model to polymicrogyria needs to be experimentally verified. Patient magnetic resonance imaging (MRI) data of the cortex would allow measurements of the lateral ventricle to be obtained. If such measurements were available for healthy subjects and subjects with diseases such as polymicrogyria, realistic values for the lateral ventricle could be incorporated into our model. This would then enable our model predictions to be verified, leading to explanations of how certain cortical pattern formation disease processes develop.

In conclusion, we have presented a mathematical model that is chemically driven and offers a possible explanation as to the location of the formation of cortical folds. We modelled the lateral ventricle as a prolate spheroid and the ventricular zone as a prolate spheroidal shell. By using a BVM Turing reaction-diffusion system we have been able to make predictions as to how cortical folding may occur, including interpreting the order and directionality of folds that may form. Our results can be applied to cortical evolution as well as cortical disease processes. Our model can predict why certain species have little or no folding and it can predict why certain cortical diseases may have excessive folding. This model represents an extension of the IP model and explains consistency in cortical folding. One possible extension of our model would be to incorporate axonal tension to account for intra-species variability in cortical folding. Such an extension would link the concepts of the IP model to the axonal tension hypothesis. Our model is able to capture global shape characteristics of the cortex and represents an important step in improving our understanding of cortical folding pattern formation of the brain.

ACKNOWLEDGMENTS

REFERENCES

Barrio, R.A., C. Varea, J.L. Aragon, P.K. Maini, (1999), A two-dimensional numerical study of spatial pattern formation in interacting Turing systems. *B Math Biol*, 61, 483-505.

Colombani, M., M. Chouchane, G. Pitelet, et al., (2006), A new case of megalencephaly and perisylvian polymicrogyria with post-axial polydactyly and hydrocephalus: MPPH syndrome. *Eur J Med Gen*, 49, 466-471.

Flammer, K. (1957), Spheroidal Wave Functions. Stanford University Press, Palo Alto.

Kondo, S., R. Asai, (1995), A reaction-diffusion wave on the skin of the marine angelfish Pomacanthus. *Nature*, 376, 765–768.

Kriegstein, A., S. Noctor, V. Martinez-Cerdeno, (2006), Patterns of neural stem and progenitor cell division may underlie evolutionary cortical expansion. *Nat Rev Neurosci*, 7, 883-890.

Murray, J.D. (2003), Mathematical Biology II: Spatial Models and Biomedical Applications, Springer-Verlag, Berlin.

Noctor, S.C., V. Martinez-Cerdeno, L. Ivic, A.R. Kriegstein, (2004), Cortical neurons arise in symmetric and asymmetric division zones and migrate through specific phases. *Nat Neurosci*, 7, 136-144.

Radinsky, L. (1975), Primate brain evolution. *Am Sci*, **63**, 656-663.

Striegel, D.A. (2009), Modeling the Folding Pattern of the Cerebral Cortex. PhD Thesis, Florida State University, Tallahassee, Florida, U.S.A.

Striegel, D.A., M.K. Hurdal, (2009), Chemically-based mathematical model for evolutionary development of cerebral cortical folding patterns. Preprint.

Van Essen, D.C. (1997), A tension-based theory of morphogenesis and compact wiring in the central nervous system. *Nature*, 385, 313–318.

Varea, C., J.L. Aragon, R.A. Barrio, (1999), Turing patterns on a sphere. *Phys Rev E*, 60, 4588-4592.